Coastal Engineering 56 (2009) 166–179

Contents lists available at ScienceDirect

Coastal Engineering

journal homepage: www.elsevier.com/locate/coastaleng

Overtopping performance of different armour units for rubble mound breakwaters

T. Bruce [a,*], J.W. van der Meer [b], L. Franco [c], J.M. Pearson [d]

[a] School of Engineering and Electronics, University of Edinburgh, King's Buildings, Edinburgh, EH9 3JL, United Kingdom
[b] Van der Meer Consulting B.V., P.O. Box 423, 8440 AK, Heerenveen, The Netherlands
[c] Univer2sity of Rome 3, Dept. Civil Eng., Via V.Volterra 62, 00146 Roma, Italy
[d] University of Warwick, School of Engineering, Coventry, CV4 7AL, United Kingdom

ARTICLE INFO

Available online 12 June 2008

Keywords:
Rubble mound breakwaters
Overtopping
Armour blocks
Wave reflection
Armour roughness
Overtopping volumes
Mean overtopping discharge

ABSTRACT

This paper describes a major programme of small-scale physical model tests to establish better the influence of armour type and configuration on overtopping. Specifically, 179 tests determined the relative difference in overtopping behaviour for 13 types/configurations of armour. Roughness factors γ_f were determined for rock (two layers), cubes (single layer and two layers), Tetrapod, Antifer, Haro, Accropode, Core-Loc™ and Xbloc™. These roughness influence factors have been included in the *CLASH* database and are for use in the neural network prediction of overtopping. Individual wave-by-wave overtopping volumes were analysed and found to compare well with current prediction methods. Measured reflection coefficients for the different units are also presented and compared with recent formulae.

1. Introduction

The overtopping database of the *CLASH* project (Steendam et al., 2004) contains more than 10,000 test results on wave overtopping at coastal structures worldwide and is therefore considerably larger than initially foreseen. The database was used as input for a neural network which resulted in a generic prediction method for overtopping at coastal structures (Pozueta et al., 2004; Van der Meer et al., 2005b).

Interim analysis of the overtopping database indicated that there were some "white spots" where further model tests would be advantageous. Test programmes to fill these "white spots" were devised. This paper describes a major programme of 2D physical model tests to establish better the influence of armour roughness on overtopping. Specifically, the objective was to determine the relative difference in overtopping behaviour for various types of armour units leading to roughness factors γ_f for the database and for use in the neural network prediction of overtopping. In addition to measurements of mean overtopping discharge, wave-by-wave overtopping volumes and reflection characteristics were also measured and compared with prediction tools.

2. Technical background

2.1. Run-up and overtopping at sloping structures

Wave run-up has always been less important for rock slopes and rubble mound structures and the crest height of these type of structures has mostly been based on allowable overtopping, or even on allowable transmission (low-crested structures). Still an estimation or prediction of wave run-up is valuable as it gives a prediction of the number or percentage of waves which will reach the crest of the structure and eventually give wave overtopping. This number is needed for a good prediction of individual overtopping volumes per wave.

Fig. 1 gives 2% wave run-up heights for various rocks slopes with cot α=1.5, 2, 3 and 4 and for an impermeable and permeable core of the rubble mound. These run-up measurements were performed during the stability tests on rock slopes of Van der Meer (1988a). First of all the graph gives values for a large range of the breaker parameter $\xi_{m-1,0}$ due to the fact that various slope angles were tested, but also with long wave periods (giving large $\xi_{m-1,0}$ values). Most breakwaters have steep slopes of 1:1.5 or 1:2 and thus the range of breaker parameters is often limited to $\xi_{m-1,0}$=2–4. The graph gives rock slope information outside this range, which may be useful also for slopes with concrete armour units.

The prediction for the 2% wave run-up value for rock slopes for $\xi_{m-1,0} \le 1.8$ can be described by (EurOtop, 2007):

$$\frac{R_{u2\%}}{H_{m0}} = 1.65\gamma_b\gamma_f\gamma_\beta\xi_{m-1,0} \quad \xi_{m-1,0} \le 1.8 \tag{1}$$

with a maximum of

$$\frac{R_{u2\%}}{H_{m0}} = 1.00\gamma_b\gamma_{f,\mathrm{surging}}\gamma_\beta\left(4.0 - \frac{1.5}{\sqrt{\xi_{m-1,0}}}\right) \quad \xi_{m-1,0} \le 1.8 \tag{2}$$

* Corresponding author.
E-mail address: Tom.Bruce@ed.ac.uk (T. Bruce).

0378-3839/$ – see front matter © 2008 Elsevier B.V. All rights reserved.
doi:10.1016/j.coastaleng.2008.03.015

Notation

α angle of foreshore slope (measured from horizontal)
γ_β influence factor for effect of oblique wave attack
γ_b influence factor for effect of a berm
γ_f influence factor for effect of slope roughness
γ_h influence factor for effect of a shallow foreshore
Δ relative buoyant density of armour unit $(=\frac{\rho_{\text{unit}}}{\rho_{\text{water}}}-1)$
ϕ armour unit packing density (no. of units per square D_n)
ρ_{water}; ρ_{unit} density of water; density of armour unit [kg/m^3]
$\xi_{m-1,0}$ breaker (or surf-similarity) parameter based upon $T_{m-1,0}$ $(=\frac{\tan\alpha}{\sqrt{s_{m-1,0}}})$
ξ_p breaker (or surf-similarity) parameter based upon T_p $(=\frac{\tan\alpha}{\sqrt{s_{\text{op}}}})$
a Weibull scale parameter, and (scaling) fitting coefficient for new formula for K_r
b Weibull shape parameter, and (shape) fitting coefficient for new formula for K_r
B_t breadth of toe of structure [m]
D_n armour unit nominal diameter $\left(=\left(\frac{\text{unit mass}}{\rho_{\text{unit}}}\right)^{1/3}\right)$ [m]
D_{n50}; D_{n85}; D_{n15} median; 85% and 15% non-exceedance values of D_n [m]
g acceleration due to gravity [m/s^2]
G_c crest width of the structure [m]
h_s water depth at toe of structure [m]
H_0 design wave height (*i.e.* maximum H_{m0} for design of armour) [m]
H_{m0} significant wave height obtained from spectral analysis $(=4\sqrt{m_0})$ [m]
H_{si} significant wave height of incident waves at the structure [m]
K_r reflection coefficient (from structure)
k_t layer thickness coefficient
N total number of armour units deployed
N_a number of armour units per m^2 per layer
P_V probability that a particular overtopping event volume exceeds V
q (dimensional) mean overtopping discharge [m^3/s/m]
R_c crest freeboard [m]
$R_{u2\%}$ wave run-up, 2% exceedance level [m]
$s_{m-1,0}$ wave steepness based upon period $T_{m-1,0}$
s_{op} wave steepness based upon offshore peak period
$T_{m-1,0}$ mean wave period obtained from spectral analysis $(=m_{-1}/m_0)$ [s]
T_p spectral peak wave period [s]
V overtopping volume associated with single overtopping event (per metre run) [m^3/m]
V_{bar} mean individual wave overtopping volume [m^3/m] (=total volume overtopping/number of overtopping events)
W_{50} median armour unit mass [kg]
$W_{\text{core,max}}$ maximum allowable mass for rock for model core [kg]
$W_{u,\text{max}}$; $W_{u,\text{min}}$ maximum; minimum allowable mass for rock for model filter layer [kg]

where γ_b, γ_f, and γ_β are influence factors accounting for berm width, armour roughness and obliquity of wave attack respectively.

For $\xi_{m-1,0}>1.8$ the roughness factor increases linearly up to 1 for $\xi_{m-1,0}=10$ and remains 1 for larger $\xi_{m-1,0}$. Over this range, the roughness influence can therefore be described by

$$\gamma_{f,\text{surging}} = \gamma_f + \frac{(\xi_{m-1,0}-1.8)(1-\gamma_f)}{8.2} \quad 1.8\leq\xi_{m-1,0}\leq 10 \tag{3}$$

$$\gamma_{f,\text{surging}} = 1.0 \quad \xi_{m-1,0}>10 \tag{4}$$

The physical explanation for this is that if the slope becomes very steep (large $\xi_{m-1,0}$ value) and the core is impermeable, the surging waves slowly run up and down the slope and all the water stays in the armour layer, leading to fairly high run-up. The surging wave actually does not "feel" the roughness anymore and behaves as a wave on a very steep smooth slope.

For steeper slopes (cot $\alpha\leq 1.5$) with a permeable core, however, a maximum is reached for $R_{u2\%}/H_{m0}=1.97$ (at $\xi_{m-1,0}\simeq 4.6$).

Eqs. (1)–(3) also give a good prediction for run-up on slopes armoured with concrete armour units, if the right roughness factor is applied.

Although there exist many formulae for the prediction of mean overtopping discharge at sloping structures, it is not the purpose of this work to evaluate these formulae. Rather, focus is on the roughness

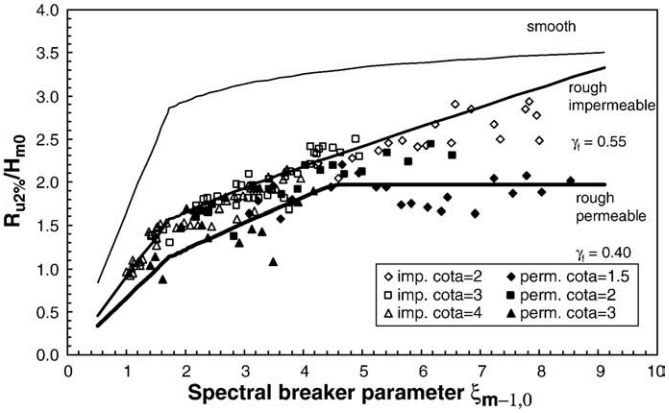

Fig. 1. Relative run-up on straight rock slopes with permeable and impermeable core, compared to smooth impermeable slopes.

Table 1
Unit properties and model/wave parameters

	W_{50} [kg]	D_{n50} [m]	D_{85}/D_{15} [–]	ρ [kg/m^3]	N_a [–]	N [–]	Δ [–]	H_0 [m]	h_s [m]	R_c [m]	B_t [m]	$W_{u,\max}$ [kg]	$W_{u,\min}$ [kg]	$W_{\text{core, max}}$ [kg]
Rock — large	0.1910	0.042	1.54	2650	398	159	1.65	0.103	0.258	0.103	0.125	0.038	0.013	0.0038
Rock — small	0.0720	0.030	1.38	2650	763	305	1.65	0.074	0.186	0.074	0.090	0.014	0.005	0.0014
Cube	0.0620	0.030		2361	660	264	1.36	0.089	0.222	0.089	0.089	0.012	0.004	0.0012
Antifer	0.0850	0.033		2361	535	214	1.36	0.099	0.247	0.099	0.099	0.017	0.006	0.0017
Tetrapod	0.1000	0.035		2350	427	171	1.35	0.104	0.259	0.104	0.105	0.020	0.007	0.0020
Accropode	0.0742	0.032		2361	622	249	1.36	0.107	0.268	0.107	0.095	0.015	0.005	0.0015
Core-Loc™	0.0605	0.030		2300	632	253	1.30	0.108	0.271	0.108	0.089	0.012	0.004	0.0012
Xbloc™	0.0620	0.030		2300	607	243	1.30	0.109	0.273	0.109	0.090	0.012	0.004	0.0012
Cubes (1 layer)	0.0620	0.030		2361	792	317	1.36	0.089	0.222	0.089	0.089	0.012	0.004	0.0012
Haro	0.0420	0.026		2361	668	267	1.36	0.092	0.231	0.092	0.078	0.008	0.003	0.0008

influence factor γ_f described above, which can also be applied to overtopping prediction, *e.g. via* Eq. (5) (TAW, 2002);

$$\frac{q}{\sqrt{gH_{m0}^3}} = 0.2\exp\left(-2.6\frac{R_c}{H_{m0}}\frac{1}{\gamma_f}\right) \tag{5}$$

In this work, the influence factor γ_f is taken to include the direct effect of armour roughness and also the effect of the armour porosity. A previous study attempted to separate out these influences on overtopping, but findings were inconclusive (Franco, 2007).

2.2. Design of a standard test situation

2.2.1. Selection of wave conditions

Large wave overtopping is often related to situations quite close to the design wave conditions for structure stability. For this study, the stability of the structure itself is not an issue. In order to compare different units of different sizes, a standard test situation and standard cross-section is required. Such a standard test situation can best be based on design conditions for the structures.

Very often breakwaters with a steep slope are designed for a fixed stability number $\frac{H_{si}}{\Delta D_n}$ where Δ is the relative buoyant density of the unit $\left(=\frac{\rho_{\text{unit}}}{\rho_{\text{water}}}-1\right)$ and D_n is the unit nominal diameter $\left(=\left(\frac{\text{unit mass}}{\rho_{\text{unit}}}\right)^{1/3}\right)$. A stability number is defined for each unit and is, then, the basis for both the test set-up and the cross-section. Further details on the design of rubble mound structures can be found in (*e.g.*) Van der Meer (1988a), and Van der Meer (1999).

Table 2 gives various units with their stability number for design — the data used for setting up and scaling of the experiments. It was originally anticipated that the model tests would include Dolosse and Shed, but unfortunately at the time of testing suitably-sized units could not be sourced.

Given the stability number, the wave height under design conditions (H_0) can be calculated. This should be a wave height which can be generated in the flume. This design wave height is given as

$$H_0 = \text{stability no.} \times \Delta D_n \tag{6}$$

Tests with $H_{m0}=H_0$ would be the maximum significant wave height for testing. Other tests should be carried out with $H_{m0}=0.5H_0$ and $0.75H_0$. Each wave height would then be repeated for three wave steepnesses, $s_{op}=0.02$, 0.035 and 0.05, where s_{op} is the nominal wave steepness $\left(=\frac{2\pi H_0}{gT_p^2}\right)$. Two water levels would be tested, giving (for most tests) $\frac{R_c}{H_0}=1.3$ and 0.8. This leads to a total of 18 tests for one structure, covering small to large overtopping. The actual number of tests however varied for each configuration.

2.2.2. Selection of standardised structure cross-section

Most structures are built in fairly shallow water, but in order to make the comparison between tests for the roughness factor easier, it is better not to include a foreshore. On the other hand, the water depth should not be too large, because the structure becomes much larger with a larger water depth. Two water depths ($2.5H_0$ and $3.0H_0$) were chosen for the tests. For such water depths the waves do not break and they can be generated without a foreshore. With focus being on the armour performance, the intention was to exclude further, complicating factors. As such, the standard structure was designed with a simple, horizontal foreshore, which was deemed acceptable as long as the water depth above it foreshore was at least $2.5H_0$.

The crest freeboard under design conditions was $1.3H_0$, giving a total structure height of $3.8H_0$. For the deeper water tests, the structure height was maintained at $3.8H_0$, with a consequent reduction in freeboard to $0.8H_0$. Fig. 2 gives the proposed standard cross-section. For the actual layer thickness, the values in Table 1 were used.

The slope of the standard structure is 1:1.5 (*i.e.* cot $\alpha=1.5$), though tests were also carried out on a 1:2 (cot $\alpha=2$) structure with rock and cube armours. All dimensions are related to H_0 or to the nominal diameter of the unit. The crest and toe are $3D_n$ wide. The under-layer

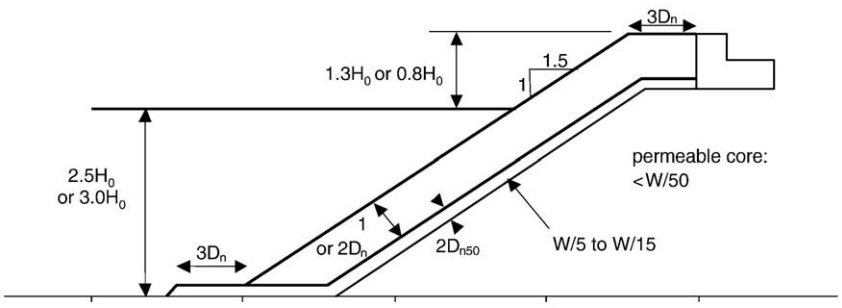

Fig. 2. Standardised cross-section for tests.

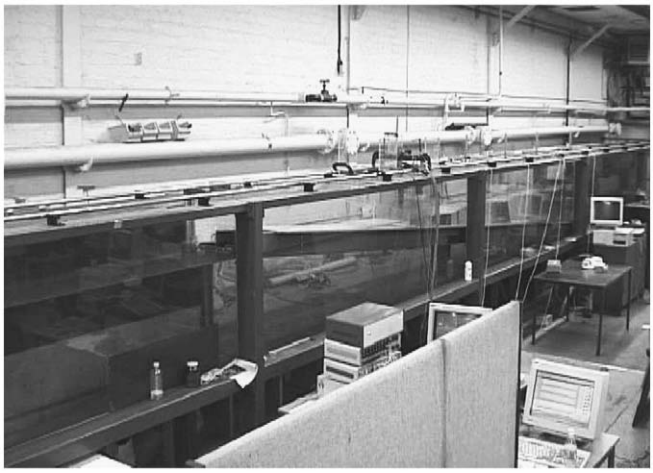

Fig. 3. General view of the Edinburgh wave flume.

was chosen to be in the range 1/5 to 1/15 of the weight of the armour unit.

3. Experimental set-up and procedure

3.1. Wave generation and measurement

The 2D experimental investigations at small-scale were all completed in the wave channel in the School of Engineering and Electronics at University of Edinburgh, UK (Fig. 3). The channel is 20 m long, 0.4 m wide and has an operating water depth of 0.7 m. The side walls and the bottom of the flume are made of glass. Waves are generated by a flap type wave paddle that is capable of generating regular and irregular waves with significant wave heights up to 0.11 m and wave periods up to 2.0 s for a fixed water depth of 0.70 m at the paddle. The paddle is equipped with active absorption which significantly reduces reflected waves returning from the structure.

Overtopping discharges were directed via a centrally-placed chute (width either 0.1 or 0.2 m), which discharged into a measuring container suspended from a load cell. Individual overtopping events were detected by two parallel strips of metal tape run along the structure crest which acted as a switch closed by the water. For higher discharge conditions, water was removed from the collection container using an electric pump during data collection periods. At the end of the test the load-cell voltage trace was passed through an algorithm which determined that total volume of water which overtopped the structure during the test. Similarly, wave-by-wave overtopping volumes were measured by determining the increment in the mass of water in the collection tank after each overtopping event following the general approach first used by Franco et al. (1994).

To determine the incident wave characteristics, three resistance-type wave gauges were used. Three gauges were positioned seaward of the structure separated by 0.75 and 0.3 m. Incident and reflected conditions were separated using the Aalborg University *WaveLab*™ software (which uses the methodology described by Mansard and Funke (1980)). The wave gauges were calibrated each morning.

Fig. 4. The model filter layer and core before armour placement.

Table 2
Stability numbers for different armour units used to scale the experiments (SPM, 1977; CLI, 2007; DMC, 2007), together with other unit data

Type of armour	$H_{si}/\Delta D_n$	No. of layers	Layer thickness coeff., k_t	Porosity (%)	Packing density, ϕ
Rock	1.5	2	1.15	~40	1.38
Cube	2.2	2	1.1	47	1.17
Antifer	2.2	2	(1.1)	(47)	(1.17)
Tetrapod	2.2	2	1.04	50	1.04
Dolosse	2.8	2	0.94	56	0.83
Accropode	2.7	1	1.51	59	0.62
Core-Loc™	2.8	1	1.51	63	0.56
Xbloc™	2.8	1	1.49	61	0.58
Cubes (1 layer)	2.2	1	1.0	30	0.70
Haro		2		51	

3.2. Structure core and filter layer

The core and filter material was graded into the correct size by sieving the material through the appropriate mesh size. For the core layer, the requirement was that the weight was less than 1/50*W*, where *W* is the weight of the armour unit. As all the armour units differed in weight, careful consideration was given such that the filter layer fitted all criteria. Fig. 4 shows the installation of the core and filter layer.

The weight difference between the different types of armour units was too large to allow a single grading of filter layer so two filter and filter layer gradings were made. The smaller grading (filter layer "A") was used for the Haro, whilst the larger grading (filter layer "B") was used for the Cubes, Antifer, Tetrapod, Rock, Core-Loc™, Accropode, and Xbloc™. Table 3 shows the core and filter layer characteristics.

The standard cross-section was inevitably the result of some degree of compromise in order that rebuilds could be kept to a minimum (maximising the available testing time). The final choice of

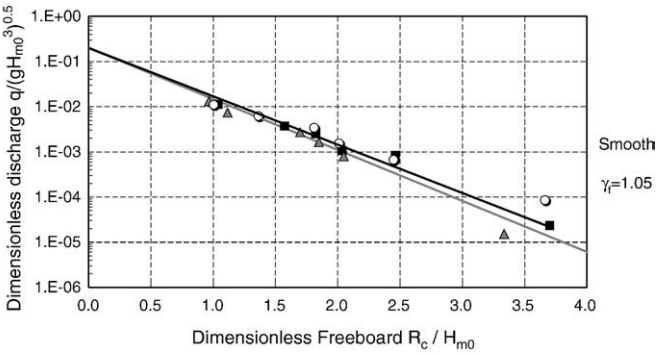

Fig. 5. Results of tests for smooth slope; cot α=1.5. Lines are best fit (γ_f=1.05, upper, black line) and γ_f=1.0 (lower, grey line). Symbols denote different nominal steepnesses; triangles, squares and circles corresponding to s_{op}~0.02, 0.035 and 0.05 respectively.

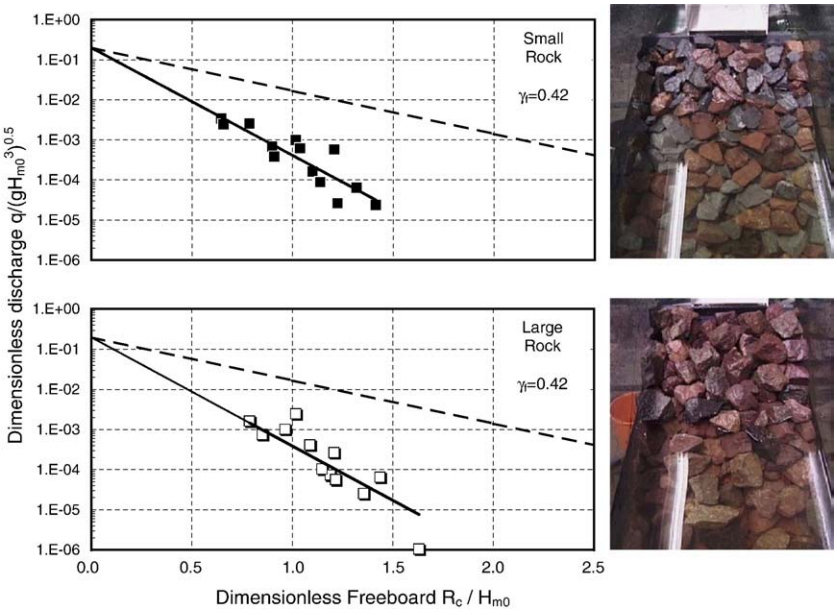

Fig. 6. Results of tests for rock; cot α=1.5 — "small" (upper graph) and "large" (lower). Dashed lines are for γ_f=1.

core material with D_n~9 mm results in a core which is marginal in terms of unwanted viscous effects and consequent concerns about this scaling effect. It is asserted, however, that because these tests are about *comparisons* between tests under a fairly narrow range of conditions whose results do not need to be scaled *per se*, any marginal viscous effects in the core will have minimal effect on the conclusions.

3.3. Testing procedure

Prior to each test, the water level was adjusted to the required freeboard (R_c). For each armour unit type, two freeboards were investigated. The size of armour unit determined the design offshore significant wave height, H_{m0}. As the units were of different size, H_{m0} also varied accordingly.

For the smooth structure, relative freeboards were R_c/H_{m0}=1.0 and 1.7. For the natural rock R_c/H_{m0}=0.9 and 1.3, and for all the other armour units R_c/H_{m0}=0.8 and 1.3.

Overtopping measurements were made at the crest wall edge. The properties of the armour units are summarised in Table 2.

The tests had a fixed duration of 1024 s and hence, depending upon the wave period, gave between 700 and 1300 waves. For all conditions a JONSWAP (γ=3.3) pseudo-random wave spectrum was used. For each armour/configuration, the packing density (number of units per square D_n), ϕ, was estimated and recorded. A summary of each set of tests for each armour unit is given on the following pages, together with graphs of overtopping data and a photograph to show the condition of the armour at the end of the tests for that structure.

For the cubes, it was decided to verify whether the placement orientation of the cube influenced the overtopping characteristics, hence the cubes were tested in a "flat" or "regular" orientation whereby the cubes were placed relatively flat to each other and the second case was when the cubes were placed in a more rough, random pattern.

4. Mean overtopping discharge

4.1. Introduction

The benchmark for the tests with different armour units was the 18 tests performed with a 1:1.5 (cot α=1.5) smooth slope, with R_c/H_{m0}=1.0 and 1.7, where R_c=110 mm and 187 mm. The data (Fig. 5) agree quite well with the Eq. (5) (TAW, 2002), though with a 5% overestimation of γ_f. It is taken that γ_f=1 is the true value, and thus all subsequent values of γ_f obtained from the experiments are reduced by this 5%.

4.2. Results — rock

For the rock tests, two stone sizes were used (Table 4). Very similar results for the different stone sizes are shown in Fig. 6.

Tests were carried out using two layers of natural rock armour on a 1:1.5 sloping structure. Relative freeboards R_c/H_{m0} were 1.3 and 0.9, with R_c=134 mm and 95 mm. The packing density ϕ was 1.38. 14 tests used "large" rock, with 15 using "small" (Table 3).

4.3. Results — cube

Tests were carried out with cubes arranged in a simple pattern with faces approximately aligned to give a smooth profile to the slope, and also with cubes arranged in an irregular or "rough" pattern. The overtopping performance of a single layer of cubes arranged in the "regular" pattern was also investigated. Results are shown in Fig. 7 which, surprisingly, showed no difference in response between "regular" and "irregular" patterns. However, compared to the equivalent double-layer pattern, the single-layer pattern produced larger overtopping discharges as expected.

Cube — double layer, "irregular" pattern: 18 tests were carried out on a 1:1.5 sloping structure armoured with two layers of cubes arranged with the faces in an irregular manner. Three tests yielded no measurable discharge. Relative freeboards were R_c/H_{m0}=1.3 and 0.8, with R_c=118 mm and 71 mm. The packing density ϕ was 1.17. Towards

Table 3
Filter and core layer characteristics

	W_{50} (g)	D_{85}/D_{15}
Core	0.86	1.30
Filter A	3.37	1.28
Filter B	7.42	1.19

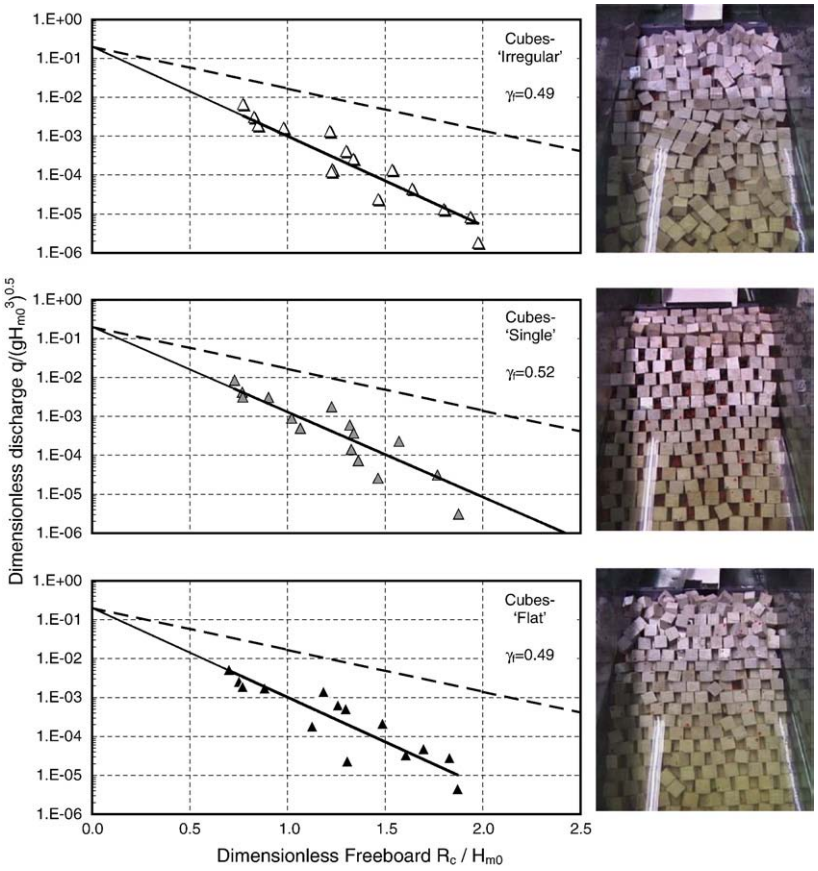

Fig. 7. Results of tests for cube — "irregular" (top graph); single layer "flat" (middle); and "flat" (bottom). Dashed lines are for $\gamma_f = 1$.

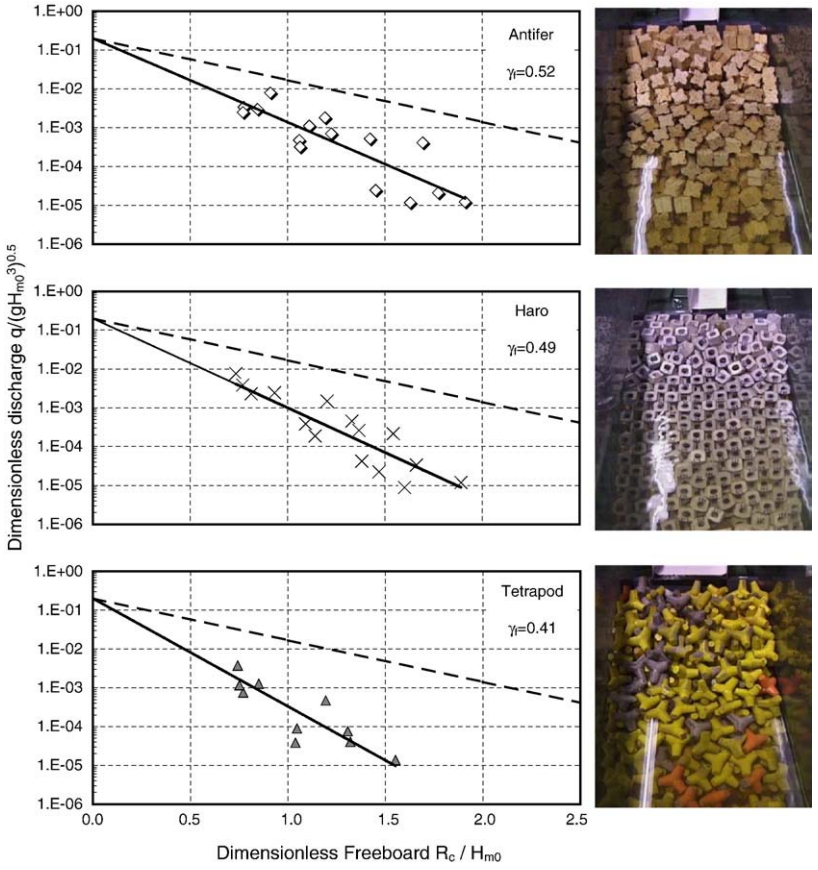

Fig. 8. Results of tests for Antifer, Haro and Tetrapod (two-layer armour systems). Dashed lines are for $\gamma_f = 1$.

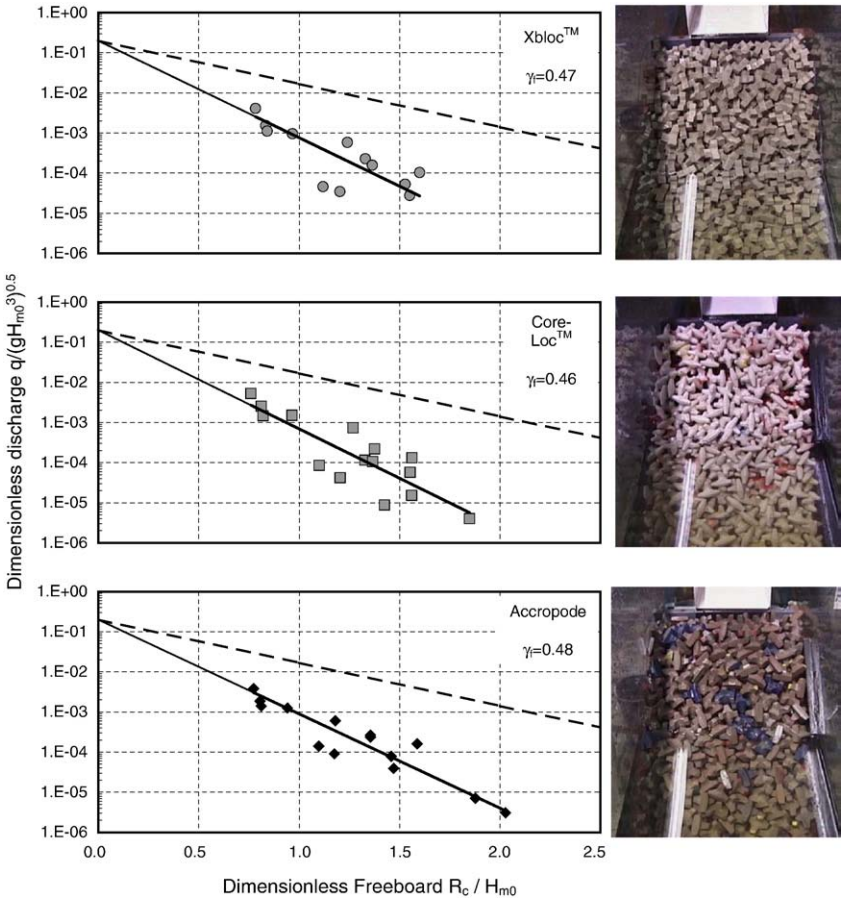

Fig. 9. Results of tests for single-layer armour systems — Accropode, Core-Loc™ and Xbloc™. Dashed lines are for $\gamma_f = 1$.

the end of the tests it was noted that the cubes moved slightly from an irregular pattern to a more regular "flat" pattern. No readjustment of the units was made during the testing.

Cube — single layer, "flat" pattern: 18 tests were carried out on a 1:1.5 sloping structure armoured with a *single layer* of cubes arranged with the faces "flat". One test yielded no measurable discharge. Relative freeboards R_c/H_{m0} were 1.3 and 0.8, with $R_c = 116$ mm and 71 mm. The packing density ϕ was 0.65.

Cube — double layer, "flat" pattern: 18 tests were carried out with cubes arranged with faces aligned flat, with three tests giving no

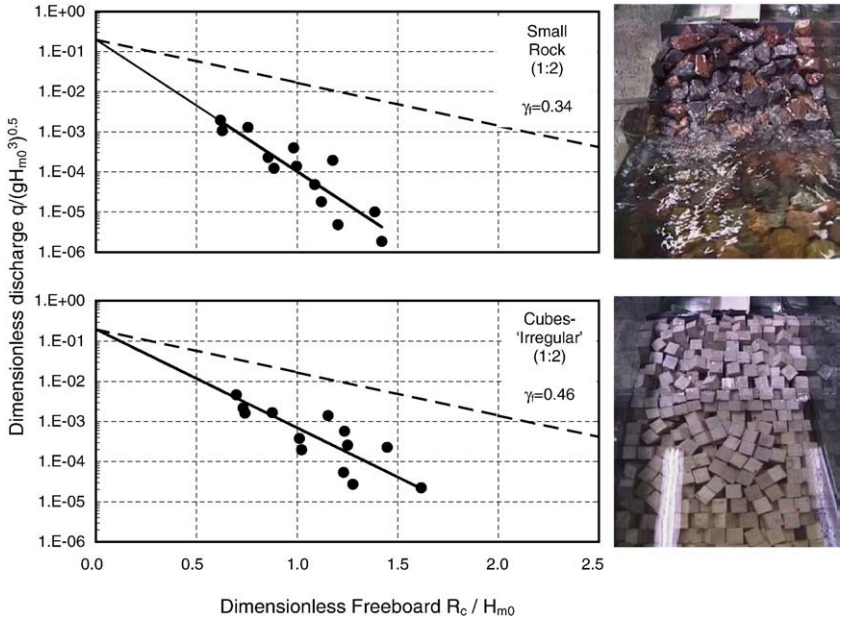

Fig. 10. Results of tests for small rock and "irregular" cubes on 1:2 slopes. Dashed lines are for $\gamma_f = 1$.

measurable discharge. Relative freeboard R_c/H_{m0} was 1.3 and 0.8, where R_c = 118 mm and 71 mm. The packing density was 1.19.

4.4. Results — other two-layer armour systems

Three other armour systems that are conventionally used as two-layer systems were tested — Antifer, Tetrapod and Haro. Data and photographs (after testing) are shown in Fig. 8.

Antifer: 18 tests were carried out on a 1:1.5 sloping structure armoured with two layers of Antifer, arranged with the faces in a regular pattern. Three of these tests gave no measurable discharge. Relative freeboards R_c/H_{m0} were 1.3 and 0.8, with R_c = 128.7 mm and 79 mm. The packing density ϕ was 1.17.

Haro: 19 tests were performed on a 1:1.5 sloping structure armoured with two layers of Haro, with faces arranged in a flat manner. Four tests gave no measurable discharge. Relative freeboards R_c/H_{m0} were 1.3 and 0.8, with R_c = 118 mm and 74 mm. Packing density ϕ was 1.16.

Tetrapod: 18 tests were performed on a 1:1.5 sloping structure armoured with two layers of Tetrapod arranged in a 'T' pattern ('SOTRAMER'). Eight of these tests yielded no measurable discharge. Relative freeboards R_c/H_{m0} were 1.3 and 0.8, with R_c = 135 mm and 83 mm.

4.5. Results — single-layer armour systems

Three armour systems that are intended for use as single-layer systems were tested — Accropode, Core-Loc™ and Xbloc™. Data and photographs (after testing) are shown in Fig. 9.

Xbloc™: 14 tests were performed on a 1:1.5 sloping structure armoured with a single layer of Xbloc™. Two tests yielded no measurable discharge. Relative freeboards R_c/H_{m0} were 1.3 and 0.8, with R_c = 142 mm and 90 mm. Packing density ϕ was 0.58.

Core-Loc™: 16 tests were performed on a 1:1.5 sloping structure armoured with a single layer of Core-Loc™. One test gave no measurable discharge. Relative freeboards R_c/H_{m0} were 1.3 and 0.8, with R_c = 86.4 mm and 140 mm. Packing density ϕ was 0.56.

Accropode: 15 tests were carried out on a 1:1.5 sloping structure armoured with a single layer of Accropode. One test gave no measurable discharge. Relative freeboards R_c/H_{m0} were 1.3 and 0.8, with R_c = 139 mm and 86 mm. The packing density ϕ was 0.62.

Additionally, a further series of single-layer armour tests were carried out with simple cubes — see Section 4.3, above.

4.6. Results — structures with 1:2 slope

Tests were also carried out on 1:2 sloped structures armoured with rock and simple (two-layer) cubes. The results are shown in Fig. 10 (upper and lower graphs/photographs respectively).

4.7. Uncertainty analysis and scale effects

In this work a total of 179 tests have been conducted over 13 different armour types/configurations (plus 18 tests with smooth slope) giving typically 14 tests per configuration. In the analysis of this data several questions need to be answered. The primary question is whether the intercept of 0.2 is truly fixed or whether instead it varies with armour type/configuration. This question is simply answered using standard statistical techniques where the intercept of the regression equation can be tested for significance. Reasonable estimates can be obtained at the 95% significance level using the analysis of variance (ANOVA) with 13 classes of *c.* 14 observations. A statistical analysis using the R statistics package (R Development Core Team, 2007) shows that there is no significant evidence to support the contention that the intercept varies with unit type, so can correctly be left at 0.2 for all configurations.

In addition to estimating the γ_f coefficient using linear regression it is possible to compute the 95% confidence interval associated with this estimate (*i.e.* the range in which we are 95% certain that the true value of γ_f lies). Table 5 shows the computed values of γ_f together with their lower and upper limits. The authors note that the 95% confidence interval for 1:2 rock lies completely outside of the remaining confidence intervals indicating that the performance of this configuration is significantly different from the others tested. Despite their overlapping confidence intervals, γ_f values for other configurations are given separately (rather than as a single, mean value) as further measurements or data from much larger data sets may improve the distinction between the unit types.

The marginal influence of scale on possible viscous effects in the core has been noted in Section 3.2. As set out in Section 2.2, the tests reported here were designed as direct comparisons of closely-related configurations. As such, for the objectives of this work, scaling of data to prototype scale (and its inherent additional uncertainty) need not follow directly. If the data were to be adjusted for model effects and scaled to prototype scale for a later purpose, the procedure given by the *CLASH* project (De Rouck et al., 2005) should be followed.

4.8. Discussion

Detailed measurements have been made in University of Edinburgh flume to parameterise the mean overtopping rates q for a range of different armour units on a 1:1.5 sloping structure. Additional investigations have been carried out on a 1:2 slope for rock, and for cube armour units. Within experimental limitations, the results demonstrate that the overtopping characteristics follow the general trend of Eq. (5) (TAW, 2002).

All lines start at R_c/H_{m0} = 0 and $q/(gH_{m0}^3)^{0.5}$ = 0.2. For smooth slopes γ_f = 1 and the value for each unit is derived by fitting a line through the data points.

Table 4
Small and large rock characteristics

	W_{50} (g)	D_{85}/D_{15}
Small rock	72	1.38
Large rock	190	1.54

Table 5
Final γ_f values for 1:1.5 sloping structures, arrived at from synthesis of new data and other comparable tests

Type of armour	No. of layers	γ_f	γ_f	γ_f
		mean	95% CI, low	95% CI, high
Smooth	–	1.00		
Rock (two layers; permeable core)	2	0.40	0.37	0.43
Rock (two layers; impermeable core)	*2*	*0.55*		
Rock (one layer; permeable core)	*1*	*0.45*		
Rock (one layer; impermeable core)	*1*	*0.60*		
Cube	2	0.47	0.44	0.50
Cube (single layer)	1	0.49	0.46	0.52
Antifer	2	0.50	0.46	0.55
Haro	2	0.47	0.44	0.50
Tetrapod	2	0.38	0.35	0.42
Accropode	1	0.46	0.43	0.48
Core-Loc™	1	0.44	0.41	0.47
Xbloc™	1	0.44	0.41	0.49
Dolosse	*2*	*0.43*		
Berm breakwater	*2*	*0.40*		
Icelandic berm breakwater	*2*	*0.35*		

Values have been normalised by comparison with smooth slope tests taken as γ_f = 1. In addition to the mean value of γ_f, values at lower and upper bounds of the 95% confidence interval (CI) are also given. Rock armour values in italics from Van der Meer (1988b). Other values in italics are estimated/extrapolated from discussion among the authors and CLASH colleagues.

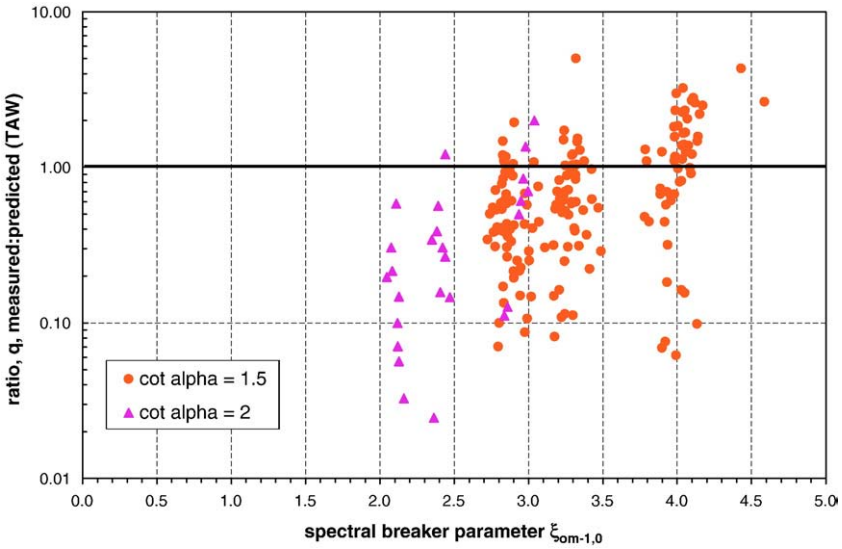

Fig. 11. Graph showing success of TAW (TAW, 2002) predictor of mean overtopping discharge as a function of breaker parameter $\xi_{m-1,0}$. All data from this study are included. 1:2 configurations are shown as triangles, with 1:1.5 data as circles.

It should be noted that Antifer were not tested in a rougher, "irregular" arrangement, which might have given a somewhat lower γ_f.

Moreover, available data from similar previous studies were re-analysed in the same way in order to optimise the final selection after joint discussions among *CLASH* partners. Specifically, Aminti and Franco (1988) (for rock, cube and Tetrapod); Franco and Cavani (1999) (for Antifer, Tetrapod and Core-Loc™); and the results of parallel *CLASH* tests undertaken at Aalborg University and at University of Ghent were reviewed and discussed. This allowed a final selection of γ_f values as given in Table 5, which are valid for a rubble mound, armoured structure with slope 1:1.5, with crest berm width $G_c = 3D_n$ with a permeable core/under-layer. Additional geometries/unit types were tentatively assigned a corresponding γ_f, based on experience from other available model tests identified within the *CLASH* overtopping database.

It is observed that the comparison with previous/parallel studies showed that for the Rock case (permeable core), γ_f varies with slope angle — Table 6. The results of this study also showed a dependency of γ_f with the slope angle for rock. In the database, and also for use of the Neural Network, only one value for γ_f is given. Thus it was noted that the Neural Network must be able to include the slope influence in its prediction. Therefore, in the database only structures with cot $\alpha = 1.5$ and $G_c = 3D_n$ should use γ_f from Table 5.

When all the mean overtopping data from this study are viewed together (Fig. 11), there emerges some indication that the success of the predictor has a weak dependency upon the breaker parameter $\xi_{m-1,0}$. Looking at the ratio, $q_{measured}$:$q_{predicted,TAW}$, a tendency for over-prediction at lower $\xi_{m-1,0}$ and for under-prediction for higher $\xi_{m-1,0}$ ($\xi_{m-1,0} \geq \sim 4$) is apparent. This trend is in line with the observations from run-up measurements that the roughness influence factor γ_f is not a fixed value for a given slope, but instead increases with $\xi_{m-1,0}$ over the range $1.8 \leq \xi_{m-1,0} \leq 10$ (see Section 2.1). This serves as a reminder that the γ_f values derived and presented in Table 5 are representative values for the range of $\xi_{m-1,0}$ covered by the tests, and further work is required to extend these boundaries to lower and higher $\xi_{m-1,0}$. It is worth noting, however, that the studied range

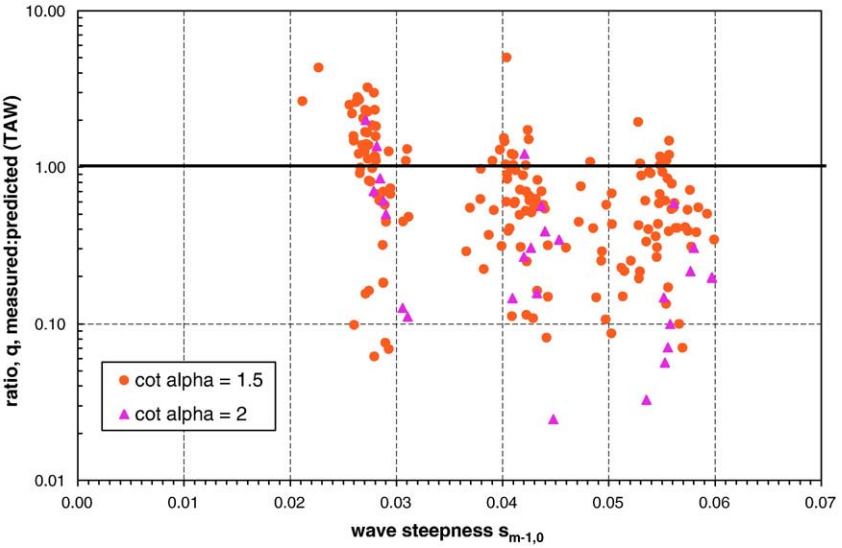

Fig. 12. Graph showing success of TAW (TAW, 2002) predictor of mean overtopping discharge as a function of wave steepness $s_{m-1,0}$. All data from this study are included. 1:2 configurations are shown as triangles, with 1:1.5 data as circles.

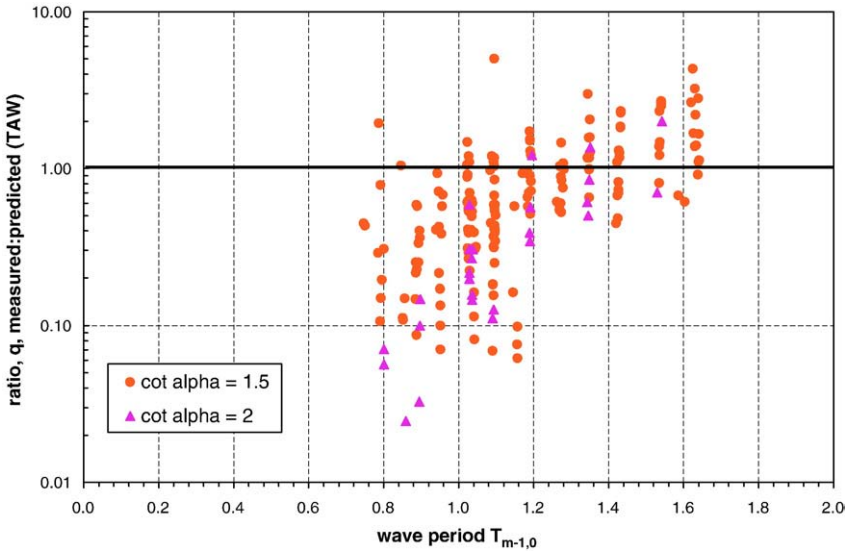

Fig. 13. Graph showing success of TAW (TAW, 2002) predictor of mean overtopping discharge as a function of wave period $T_{m-1,0}$. All data from this study are included. 1:2 configurations are shown as triangles, with 1:1.5 data as circles.

encompasses the vast majority of practical concrete armoured structures under normal operating conditions. Further, it is asserted that given the inherent scatter in overtopping data, the use of a single γ_f over the range $\sim 2.0 \leq \xi_{m-1,0} \leq \sim 4$ is acceptable for engineering assessment and design purposes.

Looking more closely at the source of the influence of breaker parameter $\xi_{m-1,0}$, it can be seen that the goodness of the fit of the data to the simple (γ_f=constant) model depends upon both incident wave steepness $s_{m-1,0}$ and wave period $T_{m-1,0}$ (Figs. 12 and 13). Both of these views are again consistent with the premise that γ_f increases (approximately linearly) with $\xi_{m-1,0}$ as *per* behaviour observed in run-up experiments (Section 2.1) with longer waves "feeling" the roughness less. Further tests will be required, however, before there would be a sufficiently substantial basis for adjusted guidance.

Looking beyond the structures tested in these studies, it is anticipated that these influence factors could also be applied in the analysis of mean overtopping discharge on steep ($\cot\alpha \leq 1.5$), armoured revetments with impermeable core.

5. Individual wave overtopping volumes

Until recently, guidance relating overtopping to direct hazard has been based upon admissible mean overtopping discharges (see *e.g.* EA, 1999). Although it has long been appreciated that individual wave overtopping volumes ought to provide a better measure of direct hazard (*e.g.* Franco et al., 1994), it is only recently that new guidance including reference to overtopping volumes has begun to emerge (Allsop et al., 2005; EurOtop, 2007). In addition to the mean overtopping discharges measured during these tests (reported in Section 4), individual, wave-by-wave overtopping volumes were also recorded throughout. Results are first presented for maximum individual overtopping volumes. It is however accepted that this is not a particularly stable measure, and

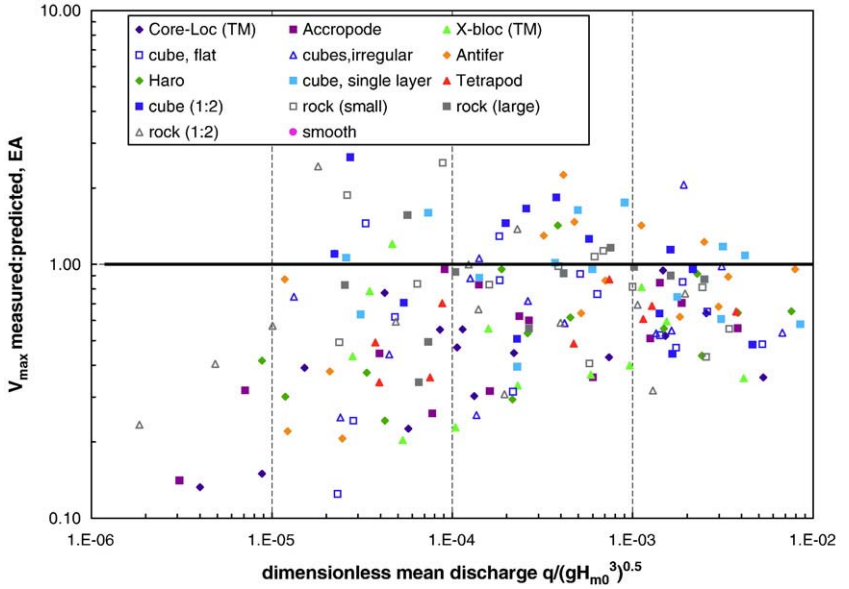

Fig. 14. Graph showing success of EA (EA, 1999) predictor of maximum individual wave overtopping volume as a function of dimensionless mean discharge.

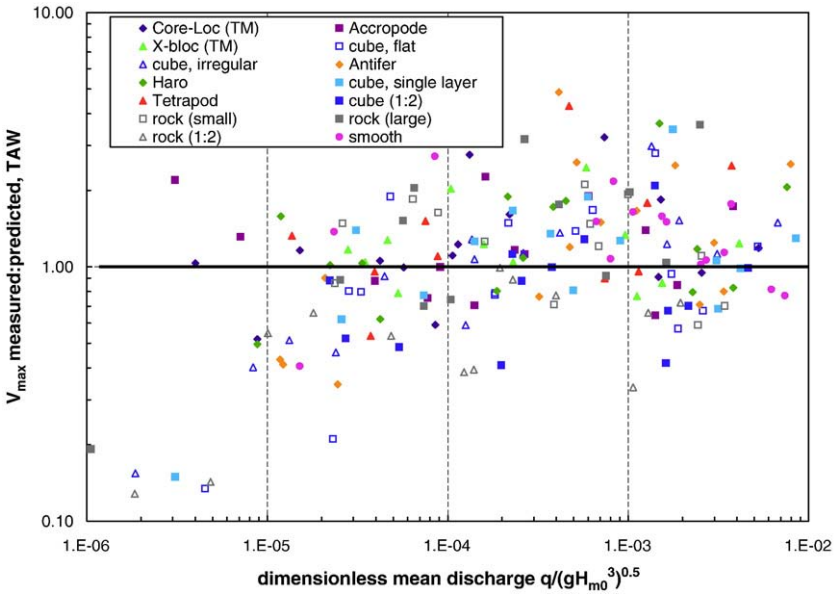

Fig. 15. Graph showing success of TAW (TAW, 2002) predictor of maximum individual wave overtopping volume as a function of dimensionless mean discharge.

results are therefore also presented comparing measured Weibull distribution parameters, with comparisons with those given in existing guidance.

Measurements of maximum individual overtopping volume are compared with those predicted by the procedures suggested by EA (1999) and TAW (2002) in Figs. 14 and 15.

While it is clear from these graphs that the EA predictor is more conservative than the TAW one which performs slightly better, both give predictions typically to within a factor of 4 over a wide range of overtopping conditions ($10^{-4}<\frac{q}{(gH_{m0}^3)^{0.5}}<10^{-2}$). For mean discharges $\frac{q}{(gH_{m0}^3)^{0.5}}<10^{-4}$, there is more scatter, though both predictors continue to give reasonable predictions. It is notable that the EA predictor gives only over-predictions (*i.e.* safe) for $\frac{q}{(gH_{m0}^3)^{0.5}}<10^{-5}$. The success of the TAW and EA procedures in giving agreement with measurements to within a factor of 4 is consistent with previous results, and the scatter is no wider than expected for such data. As no new trends are apparent, there appears to be no reason to adjust either prediction scheme on the basis of this limited data set, nor to offer any new scheme.

Recalling the influence of breaker parameter identified in Section 4.8 (Fig. 11), it is observed that a similar trend is perhaps discernible in the effectiveness of the TAW predictor (Fig. 16). Given that the scatter in the fit (measured: predicted) for individual overtopping volumes is even greater than for mean discharges, it is not felt that this possible, slight dependency on breaker parameter is of significance in engineering design/assessment over the studied range.

Although these data have shown (perhaps surprisingly) relatively modest scatter, it was considered worthwhile to go on and look at the statistical distributions of individual overtopping volumes found

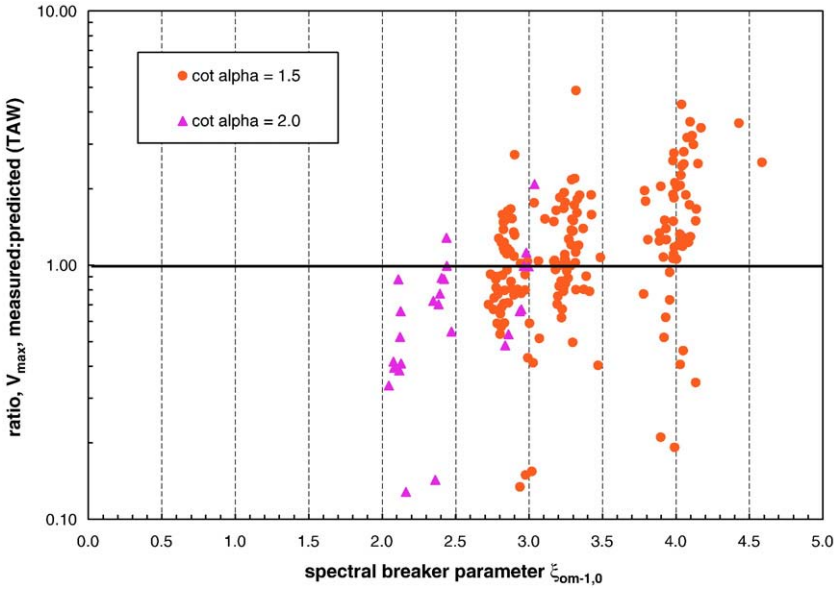

Fig. 16. Graph showing success of TAW (TAW, 2002) predictor of mean overtopping discharge as a function of breaker parameter $\xi_{m-1,0}$. All data from this study are included. 1:2 configurations are shown as triangles, with 1:1.5 data as circles.

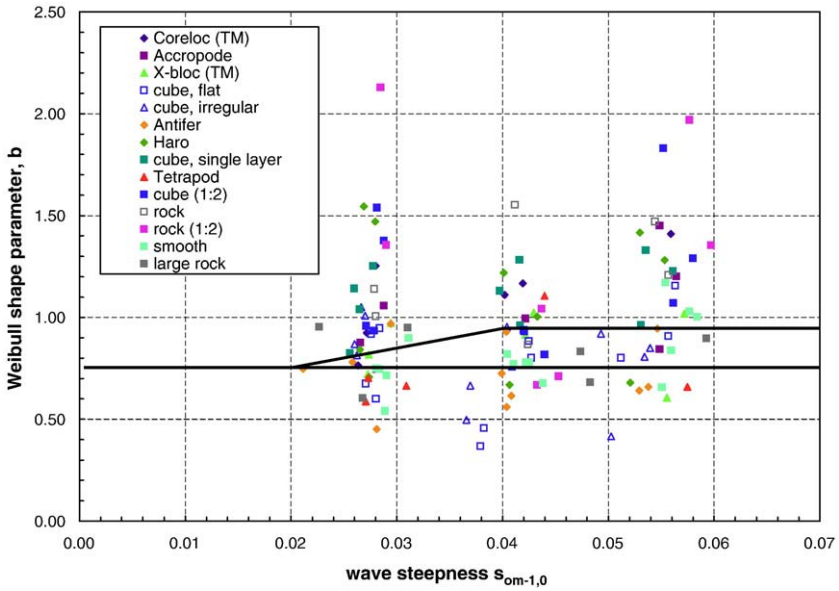

Fig. 17. Graph showing variation of measured Weibull shape parameter b with incident wave steepness. The lines indicate values suggested by TAW and EA manuals (TAW manual gives $b=0.75$ for all s_{op}; EA gives 0.76 for $s_{op}=0.02$ and 0.92 for $s_{op}=0.04$).

within each test. Previous studies have converged on the use of a two-parameter Weibull distribution as an appropriate one;

$$P_V = P(\underline{V} \leq V) = 1 - exp\left[-\left(\frac{V}{a}\right)^b\right] \quad (7)$$

where a and b are *scale* and *shape* parameters respectively. The TAW manual suggests that the shape factor (b) is taken as 0.75 for all conditions, whereas the EA Manual gives two values of b for low and high steepness incident waves.

Wave-by-wave volume data for all tests was examined, but a and b parameters were only derived for tests giving 15 or more overtopping events (≥*c.* 1.5% waves overtopping). a and b parameters are estimated by fitting the upper part of the measured distribution of individual volumes for which the volume $V \geq V_{bar}$, where V_{bar} is the average overtopping volume per overtopping wave.

Given that at least one guidance manual identifies wave steepness as having an influence on the distribution parameters, measured b values are examined as a function of incident wave steepness (Fig. 17). The principal impression from this graph is one of very great scatter and the principal conclusion must be that there is little support here for changes to existing formulations. More detailed analysis of this data suggested $b=0.74$ as a best fit, supporting the first impression that there is no new evidence to adjust existing formulations.

Whether units designed to be deployed as a single layer (here, Core-Loc™, Xbloc™ and Accropode) performed significantly differently than "conventional" two-layer systems against individual

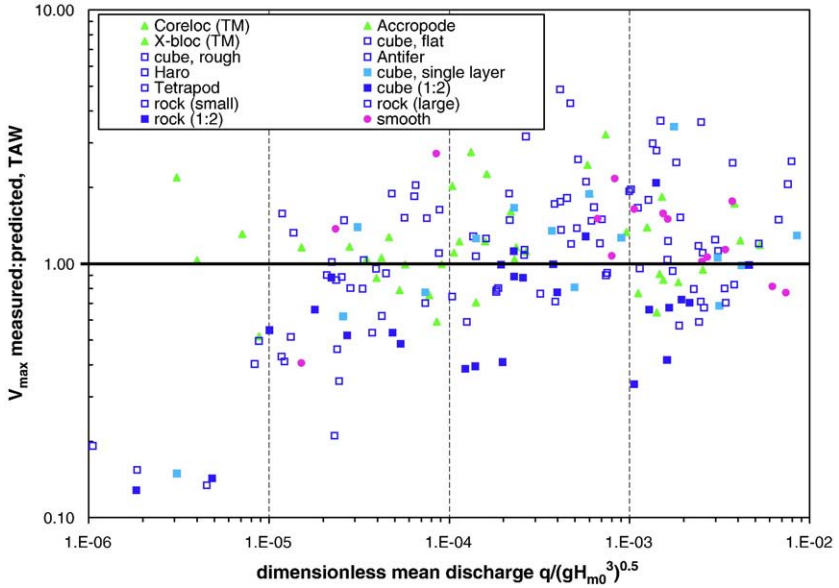

Fig. 18. Graph as *per* Fig. 15 but distinguishing single-layer systems (Core-Loc™; Xbloc™; Accropode — all shown as filled triangles) and two-layer systems (shown as open squares).

Table 6
γ_f values for rock of different slopes

Slope	γ_f
1:1.3	0.52
1:1.5	0.42
1:2	0.38
1:3.5	0.33

overtopping volumes was investigated (Fig. 18). From the graph and perhaps against expectations, it appears that for structures designed according to the standard procedure set out in Section 2.2, the single event overtopping volume response of single- and two-layer systems is indistinguishable.

6. Wave reflection

Wave conditions in the nearshore region were measured throughout all tests. WaveLab™ software (supplied by the University of Aalborg) was used to separate incident and reflected wave fields, allowing the wave reflection performance of different set-ups and armour units to be compared. A detailed literature review of previous investigations on the reflections from various type of structures, such as smooth and rock (permeable and impermeable core) slopes and slopes with artificial armour units is given by Zanuttigh and Van der Meer (2006). They also compiled data from relevant structures similar to those in this study and generated a database of some 6000 values. Included in this were part of the *DELOS* wave transmission database (Van der Meer et al., 2005a), part of the *CLASH* wave overtopping database (Steendam et al., 2004), data acquired from model testing in European facilities, field measurements (at Elmer, UK — see Davidson et al., 1996), and new tests on low-crested structures (Cappietti et al., 2006).

Zanuttigh and Van der Meer (2006) demonstrated that for analysis restricted to straight slopes data under design conditions ($R_c/H_{si} \geq 0.5$, $H_{m0}/D_{50} \geq 1.0$, $s_o \geq 0.01$, approximately 600 tests in total, with over 300 from this *CLASH* study), the presence of four "families" of data was evident: rock with a permeable core; rock with an impermeable core; smooth slopes; and slopes with armour units. Armour units fell inside the rock permeable data cloud. In their analysis of reflection coefficients K_r they considered two methodologies from the literature (Seelig and Ahrens, 1981; Postma, 1989) and went on to derive a new method.

Zanuttigh and Van der Meer (2006) derived a new formula given by

$$K_r = \tanh\left(a\xi_{m-1,0}^{b}\right) \tag{8}$$

where the calibrated values of the coefficients a and b are reported in Table 7. This formula and these values for a and b have been obtained by analysing average values of K_r by groups of $\xi_{m-1,0}$.

For the reflection measurements taken during the tests reported here, the new methodology (Eq. (8) plus Table 7) slightly overestimates K_r for armour units and rock permeable slopes for $\xi_{m-1,0} < 4$ (Fig. 19).

7. Conclusions

The roughness influence factor γ_f has been investigated experimentally *via* an extensive series of standardised tests on various concrete and rock armour systems on 1:1.5 sloping structures. Additionally, 1:2 structures armoured with rock and simple cubes were investigated. The data supported Eq. (5). New values of γ_f are presented (Table 5).

A weak influence of breaker parameter was noted, along with the established influence of structure slope. This influence is consistent with conclusions from run-up studies that the roughness influence factor γ_f increases over the range $1.8 \leq \xi_{m-1,0} \leq 10$. Specifically, reductions in overtopping discharge q of *c.* 20% and *c.* 10% were noted for rock- and cube-armoured structures respectively, when moving from 1:1.5 to 1:2 slopes.

These small-scale tests were mostly carried out on a "traditional" steep slope for which *CLASH* findings have shown a marginal scale effect (which should be treated separately). The strength of the results of this work is that they were obtained within a tightly-controlled, consistent framework of hydraulic and geometric conditions, allowing a reliable comparison of different armour performance.

It is hoped that further tests could be performed, possibly at large-scale, to extend the validity of the results and reduce the associated uncertainties. In particular, a study focussed on the effects of slope angle, permeability of underlayers and effect of crest berm would be of great value. Experiments to try to decouple the effects of roughness and porosity would give valuable insight into the physical processes underpinning this area of research.

Individual maximum overtopping volumes are reasonably well predicted by the formulae offered by TAW (2002) and EA (1999), with predictions typically in agreement with measurements to within a

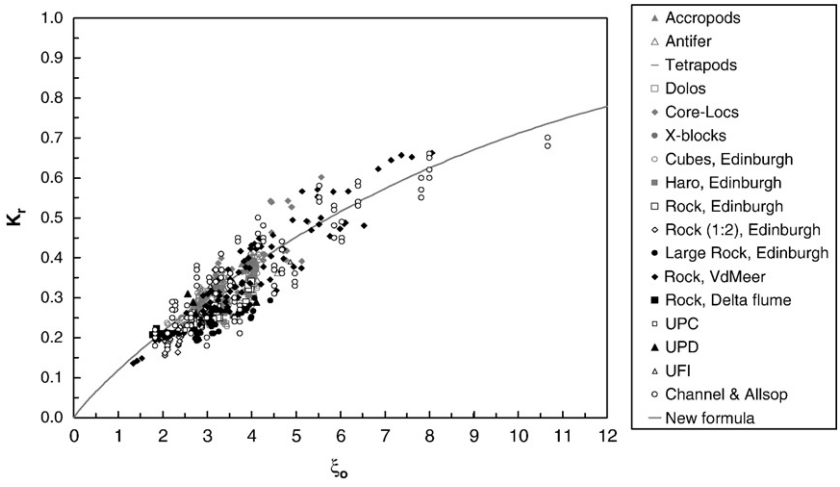

Fig. 19. Rock permeable (black points) and armour unit slopes (grey points) and the Zanuttigh and Van der Meer (2006) formula — coefficients in Table 7.

Table 7
Coefficients a and b for Eq. (8)

	a	b	γ_f
Rock (permeable)	0.12	0.87	0.40
Rock (impermeable)	0.14	0.90	0.55
Armour units	0.12	0.87	Various
Smooth	0.16	1.43	1.00

factor of 4 for dimensionless mean discharges greater than 10^{-4}. Weibull analysis of the distribution of individual volumes within each sea state does not provide evidence for any adjustment to existing guidance as offered (slightly differently) by TAW (2002) and EA (1999).

Wave reflection coefficient measurements taken in front of the sloping, armoured structures tested in this work are found to be in good agreement with the new prediction method given by Zanuttigh and Van der Meer (2006), with a slight tendency to over-prediction being observed.

Acknowledgements

The investigations in this study have only been possible by the very kind support and assistance given by the following organisations, who supplied some of the model units:

Sogreah, France (Accropode and Core-Loc™); Delta Marine Consultants bv, The Netherlands (Xbloc™); Protecno, Italy (Tetrapod); Flanders Hydraulics, Belgium (Antifer).

The use of WaveLab 2.6, supplied by the University of Aalborg, is gratefully acknowledged for additional analysis of the wave conditions.

The support of the European Community Fifth Framework under Project Code EVK3-CT-2001-00058 is also gratefully acknowledged.

The authors are very grateful to David Ingram (University of Edinburgh), who kindly carried out the statistical significance testing of the data.

Marco Falzacappa and Roberto Molino, recent graduates from the University of Roma 3, ably supported model testing at Edinburgh and subsequent analysis in Rome. Their most helpful contribution is gratefully acknowledged.

The Edinburgh team acknowledge the support of the Scottish Funding Council for the Joint Research Institute with the Heriot-Watt University which is a part of the Edinburgh Research Partnership.

References

Allsop, N.W.H., Franco, L., Bellotti, G., Bruce, T., Geeraerts, J., 2005. Hazards to people and property from wave overtopping at coastal structures. In: Proc. International Conference on Coastlines, Structures and Breakwaters 2005. ICE, Thomas Telford, London, pp. 153–165, ISBN 0-7277-3455-5.

Aminti, P., Franco, L., 1988. Wave overtopping on rubble mound breakwaters. In: Proc. 21st International Conference on Coastal Engineering. ASCE, ASCE, New York, pp. 770–781.

Cappietti, L., Clementi, E., Aminti, P., Lamberti, A., 2006. Piling-up and filtration at low crested breakwaters of different permeability. Proc. 30th International Conference on Coastal Engineering. ASCE, World Scientific, Singapore, pp. 4957–4969. ISBN-13 978-981-270-636-2.

CLI, 2007. Concrete Layer Innovations. www.concretelayer.com (accessed October 2007).

Davidson, M.A., Bird, P.A.D., Bullock, G.N., Huntley, D.A., 1996. A new non-dimensional number for the analysis of wave reflection from rubble mound breakwaters. Coastal Engineering 28, 93–120.

De Rouck, J., Geeraerts, J., Troch, P., Kortenhaus, A., Pullen, T., Franco, L., 2005. New results on scale effects for wave overtopping at coastal structures. In: Proc. International Conference on Coastlines, Structures and Breakwaters 2005. ICE, Thomas Telford, London, pp. 29–43, ISBN 0-7277-3455-5.

DMC, 2007. Delta Marine Consultants b.v. www.xbloc.com (accessed October 2007).

EA, 1999. In: Besley, P. (Ed.), Overtopping of Seawalls: Design and Assessment Manual. The Environment Agency, UK. ISBN1 85705 069 X.

EurOtop, 2007. EurOtop — Wave Overtopping of Sea Defences and Related Structures: Assessment Manual. Environment Agency (UK), Expertise Netwerk Waterkeren (NL), Kuratorium fr Forschung im Ksteningenieurwesen (DE), Pullen, T., Allsop, N.W.H., Bruce, T., Kortenhaus, A., Schüttrumpf, H. and van der Meer, J.W.; www.overtopping-manual.com.

Franco, L., 2007. private communication.

Franco, L., Cavani, A., 1999. Overtopping response of core-locs, tetrapods and antifer cubes. Proc. Coastal Structures '99. A.A. Balkema, Rotterdam, pp. 383–387. ISBN 90 5809 092 2.

Franco, L., de Gerloni, M., van der Meer, J.W., 1994. Wave overtopping on vertical and composite breakwaters. In: Proc. 24th International Conference on Coastal Engineering. ASCE, ASCE, New York, pp. 1030–1044, ISBN 0-7844-0089-X.

Mansard, E.P.D., Funke, E.R., 1980. Measurement of incident and reflected spectra using a least squares method. National Conference Publication — Institution of Engineers, Australia, n.80/1, pp. 95–96.

Postma, G.M., 1989. Wave reflection from rock slopes under random wave attack. Master's thesis, Delft University of Technology.

Pozueta, B., van Gent, M.R.A., van den Boogaard, H.F.P., Medina, J.R., 2004. A neural network modelling of wave overtopping at coastal structures. In: Proc. 29th International Conference on Coastal Engineering. ASCE, World Scientific, Singapore, pp. 4275–4287, ISBN 981-256-298-2.

R Development Core Team, 2007. R: A Language and Environment for Statistical Computing. R Foundation for Statistical Computing, Vienna, Austria. ISBN 3-900051-07-0, www.R-project.org.

Seelig, W.N., Ahrens, J.P., 1981. Estimation of wave reflection and energy dissipation coefficients for beaches, revetments and breakwaters. Tech. Rep., vol. 81-1. U.S. Army Corps of Engineers Coastal Research Center.

SPM, 1977. Shore Protection Manual. United States of America, 3rd Edition. Army Coastal Engineering Research Center, Fort Belvoir.

Steendam, G.-J., van der Meer, J.W., Verhaeghe, H., Besley, P., Franco, L., van Gent, M.R.A., 2004. The international database on wave overtopping. In: Proc. 29th International Conference on Coastal Engineering. ASCE, World Scientific, Singapore, pp. 4301–4313, ISBN 981-256-298-2.

TAW, 2002. In: van der Meer, J.W. (Ed.), Technical Report on Wave Run-up and Wave Overtopping at Dikes. Technical Advisory Committee on Flood Defence, The Netherlands. www.tawinfo.nl.

Van der Meer, J.W., 1988a. Deterministic and probabilistic design of breakwater armor layers. J. Waterway, Port, Offshore and Coastal Engineering 114 (1), 66–80.

Van der Meer, J.W., 1988b. Rock slopes and gravel beaches under wave attack. Ph.D. thesis, Delft University of Technology, (also Delft Hydraulics Publications no.396).

Van der Meer, J.W., 1999. Design of concrete armour layers. Proc. Coastal Structures '99. A.A. Balkema, Rotterdam, pp. 213–221. ISBN 90 5809 092 2.

Van der Meer, J.W., Briganti, R., Zanuttigh, B., Wang, B., 2005a. Wave transmission and reflection at low crested structures: design formulae, oblique wave attack and spectral change. Coastal Engineering 52 (10–11), 915–929.

Van der Meer, J.W., van Gent, M.R.A., Pozueta, B., Vergaege, H., Steendam, G.-J., Medina, J.R., 2005b. Applications of a neural network to predict wave overtopping at coastal structures. In: Proc. International Conference on Coastlines, Structures and Breakwaters 2005. ICE, Thomas Telford, London, pp. 259–268, ISBN 0 7277 3455 5.

Zanuttigh, B., Van der Meer, J.W., 2006. Wave reflections from coastal structures. In: Proc. 30th International Conference on Coastal Engineering. ASCE, World Scientific, Singapore, pp. 4337–4349, ISBN-13 978-981-270-636.